Waveguide Photonic Choke Joint with Wide Out-of-band Rejection

Kongpop U-yen and Edward J. Wollack
NASA Goddard Space Flight Center
Greenbelt, Maryland, USA
Kongpop.u-yen-1@nasa.gov

***Abstract*— A photonic choke joint structure with a wide- stop-band is proposed for use as a waveguide flange interface. The structure consists of arrays of square metal pillars arranged in a periodic pattern to suppress the dominant-mode wave propagation in parallel-plate waveguide over a wide frequency bandwidth. The measurement results at microwave frequencies confirm the structure can provide broadband suppression, more than 56 dB over 6.25 times its operating frequency. Applications at millimeter wavelength are discussed.**

Keywords—frequency selective surfaces, microwave filters, microwave devices, waveguide junctions, surface waves.

I. INTRODUCTION

Photonic or meta-material structures are widely used in controlling the propagation of light [1-3]. In microwave applications, such structures can be realized from sub-wavelength dielectric or metallic pillars arranged in a periodic pattern. The method of images enables one to view such a structure as an artificial dielectric [4]. For interfacing with a parallel-plate planar waveguide, these posts are arranged in a two-dimensional tiling between flat conducting metal surfaces as shown in Fig. 1. Two metal surfaces behave as mirrors for the periodic posts, imitating an imaginary three-dimension tiling observed by an incident electromagnetic wave by symmetry. The size and shapes of the pattern determine the operating frequency band where the signal is reflected and behaves as a band-stop filter [5-7]. This can be used as a part of the waveguide interface for low loss power transmission without physical contact. This unique feature allows the waveguide to be operated with a large temperature gradient between the transmission line's opposing conductors. In addition, the spacing between conductors can be used for housing planar circuitry [8].

In previous work [5], the dual-polarized waveguide photonic choke joint (PCJ) realized with square conductive pillars is optimally designed to provide stop-band over a limited range of operating frequencies. However, above the signal band, the wavelength becomes small relative to the pillar size and spacing allowing undesired propagation through the PCJ structure. This is demonstrated in ANSYS High Frequency Structural Simulator (HFSS) for an infinitely wide pillar array for X-band waveguide flange applications shown in Fig 2(a) where two metal surfaces are separated by two dielectrics, with the thickness of t_1 and t_2. Perfect magnetic walls are used as a boundary condition to mimic the effect of an infinitely wide

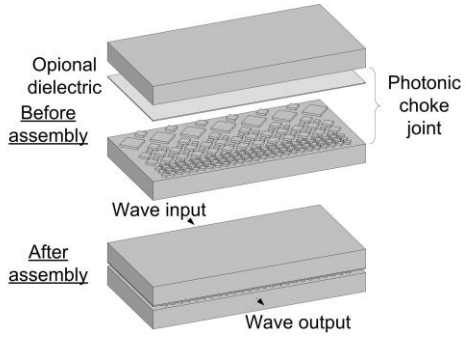

Fig. 1. The photonic choke joint with wide out-of-band rejection.

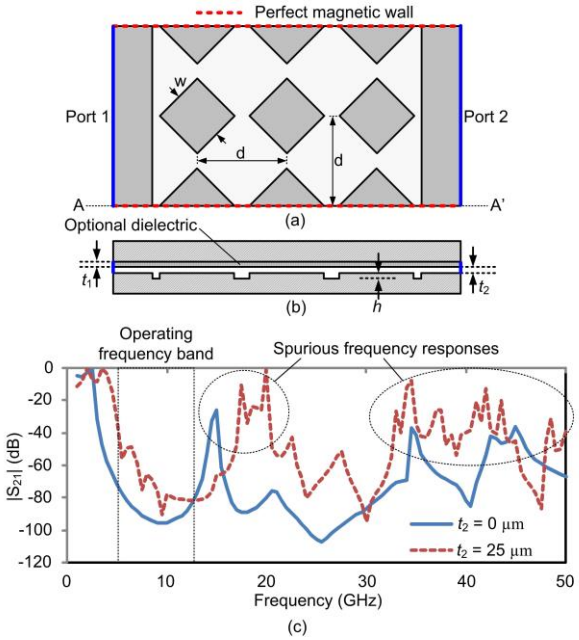

Fig. 2. A model to demonstrate spurious responses generated by a PCJ with a conventional Cartesian tiling pattern [5] when excited by plane wave (a) top view, (b) cross- sectional view A-A' and (c) simulated power transmission response (S_{21}) with optional Polyflon Cuflon (with dielectric constant of 2.05), spacer thickness t_1 of 25μm between two conductors and with the pillar height h of 0.762mm.

tiling and a plane wave is launched into the dielectric space between two conductor surfaces as shown in Fig. 2(b). By sending a plane wave signal into port 1 and receiving at port 2,

one observes spurious responses out of operating frequency band as shown in Fig. 2(c).

In this paper, we propose to use a series of PCJ with various pillar sizes and spacings to extend its out-of-band rejection capabilities for waveguide flange applications. Optimal PCJ configurations are studied in Section II. Furthermore, performance limitations on verifying its suppression capabilities are addressed in Section III. The hardware implementation and measurements are discussed in Section IV. Finally, the proposed structure is implemented in waveguide flange in Section V.

II. OPTIMAL PHOTONIC CHOKE JOINT CONFIGURATIONS

To increase the reject-band of the PCJ, square pillar arrangements with a variety of sub-array spacings and sizes were studied. Two pillars arrangements were proposed where pillars were connected in series from large to small size as shown in Fig. 3(a) and 3(b). The largest and the smallest pillar size define the lower and the upper edge of the stop-band, respectively. The optimized pillar width (w) and spacing (d) of 0.4a and 0.68a defined in [5] were used in this paper, respectively. The width a of the waveguide broadwall is 17.15mm for the PCJ designed with the center operating frequency of 8 GHz. The optimal pillar height (h) is set at 0.762 mm. The simulation model of the proposed PCJ was constructed similar to that mentioned in Section I to verify its out-of-band rejection capability. Simulation results in Fig. 4 show that the PCJ arranged in version 1 using five pillar rows can produce more than 50 dB of attenuation up to more than seven times its operating frequency.

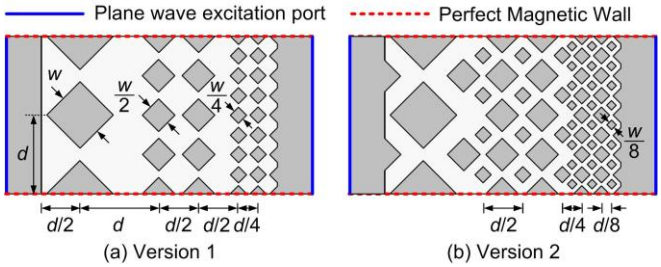

Fig. 3. The top surface of the unit cell of the proposed Cartesian tiling PCJ with w = 6.858mm and d = 12.07mm – (a) version 1 and (b) version 2.

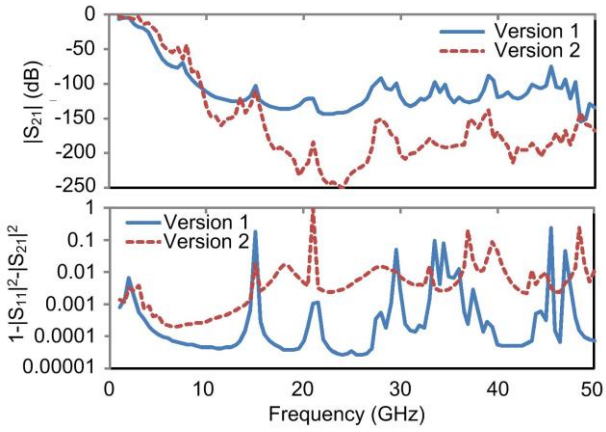

Fig. 4. The simulated power transmission (S_{21}) and power absorption (1-$|S_{11}|^2$-$|S_{21}|^2$) responses of two optimal PCJs with the dielectric spacing of t_1=25μm and t_2=0μm.

The out-of-band rejection performance of PCJ version 1 can be significantly improved by introducing additional metallic pillars in PCJ version 2. An additional out-of-band power rejection of 40 dB was observed in modeling. The absorptive loss (1-$|S_{11}|^2$-$|S_{21}|^2$) shown in Fig. 4 was due to loss in Polyflon Cuflon dielectric (with loss tangent of 0.00045) presence in the PCJ structure. For this infinite array tiling and we adopted this variation for more refined study.

III. PCJ SUPPRESSION PERFORMANCE LIMITATIONS

Although the theoretical designs discussed in Section II can achieve high-suppression level over broad frequency ranges, the physical verification of its out-of-band rejection can be challenging. Its performance is limited by the structure not being infinitely wide or when two conductor flanges are not brought into electrical contact. By modeling the proposed PCJ (see Fig. 5), one observes that the electric fields can propagate around the dielectric and air surrounding a finite section of tiling. Dependent on the width of the PCJ structure relative to the width of the microstrip port, the power leakage can vary significantly as shown in Fig. 6.

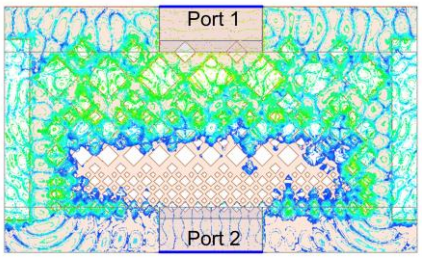

Fig. 5. Simulated electric field in the dielectric at 50 GHz shows the leakage around the 7·d-wide PCJ (version 2) with t_1=25μm and t_2=0μm.

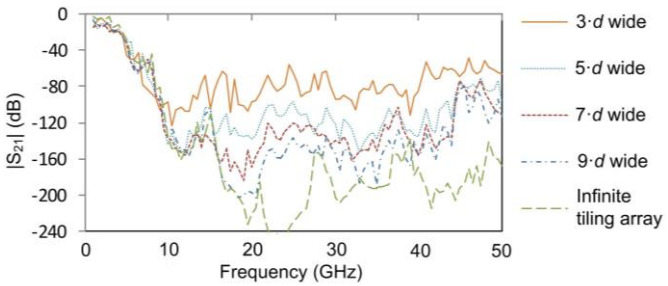

Fig. 6. The simulated power transmission of the PCJ (version 2) with a finite number of pillar rows in comparison with the an infinite tiling array case. The microstrip ports are 2·d wide.

IV. HARDWARE IMPLEMENTATION AND TEST

A prototype of PCJ (version 2; 7·d wide) was constructed to verify its ability to suppress plane-wave propagation as shown in Fig. 7 (a). The PCJ with 7·d wide is chosen as it provides sufficient approximation of an infinite array as described above. Verification of the stop-band over a broad bandwidth and dynamic range at mm-wave frequencies is experimentally challenging [2-3]. In measuring the isolation arising from the PCJ it is necessary to efficiently launch the mode, which is of interest for the end use. Here we develop and present a method of coupling to, measuring, and calibrating the observations which explicitly accounts for the embedding environment. To

appropriately excite the PCJ and calibrate for line losses, various broadband microstrip impedance transformers on 25.4µm-thick Polyflon Cuflon dielectric were designed and fabricated. Their arrangements in the back-to-back configuration are shown in Fig. 7(b-e).

The microstrip impedance transformers in Fig. 7(b), 7(c) and 7(e) transforms a 50 Ohm line into a 0.4 Ohm line by splitting 50 Ohm line into eight sections and combining them in-phase and in parallel to approximate plane-wave transmission. In this approach, the 50 Ohm line input is first transformed to a 3.2 Ohm line in the first stage. Then, the 3.2 Ohm line is split into a pair of 6.4 Ohm lines in parallel and transformed back to 3.2 Ohm line impedances. The power split process is repeated in three-stage binary tree configuration to allow only single-mode propagation through the 2.28mm-wide microstrip line up to 48 GHz. This similar approach was also used in high voltage nanosecond-pulse transmission application [9]. The continuous optimal impedance taper transformer profile [10] was used in this design to minimize the total length as well as to eliminate discontinuity in the line width. The measurement result in Fig. 8 shows that this transformer can provide low transmission-ripple for the PCJ measurement from 7 to 50 GHz, while two narrower microstrip transformer designs combined back-to-back (shown

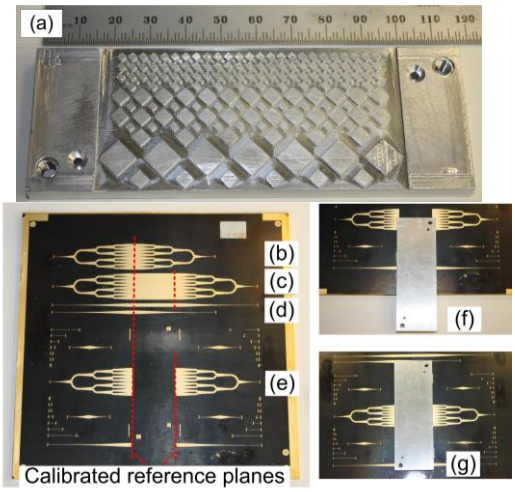

Fig. 7. Fabricated PCJ (a), impedance transformers on 25.4µm-thick Polyflon Cuflon substrate (b-e) and the PCJ placement facing of the substrate (f) and (g) for quasi-TEM and pseudo plane-wave mode measurement, respectively.

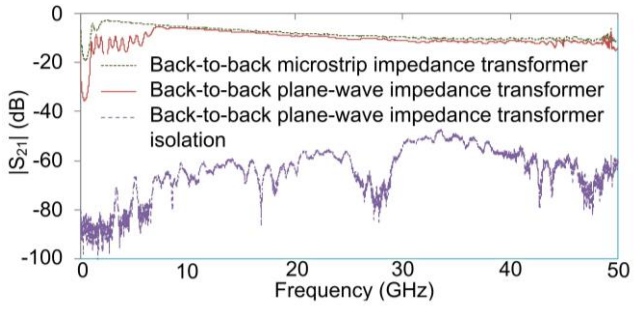

Fig. 8. The measured transmission response of the microstrip line (Fig. 7(d)) and (pseudo) plane-wave (Fig. 7(c)) impedance transformer combined back-to-back. The measured isolation between two (pseudo) plane wave ports was obtained using the planar circuit in Fig. 7(e).

Fig. 7(d)) were used for transmission line calibration between 2 and 7 GHz.

To characterize transmission response, the PCJ was placed on top of the dielectric between two impedance transformers and were symmetrically aligned as shown in Fig. 7(f) and 7(g). The signal was transmitted and received through a microstrip line using Cascade Infinity probes I50-A-GSG-250. The measurement was performed using Agilent vector network analyzer N5245A and was calibrated at the microwave probe tips using Short-Open-Load-Thru calibration standard substrate. The PCJ can provide more than 56 dB of suppression from 12 GHz to 50 GHz when the PCJ is ~ 12.5µm away from the dielectric substrate, as shown in the measurement results in Fig. 9. The observed DC resistance between two ports of 0.4 Ohm which has negligible influence on the microwave response.

As the flange conductor spacing (t_2) increases, spurious response occurred resulting in lower isolation as anticipated and observed in modeling. To measure the PCJ response below 7 GHz, the PCJ was placed symmetrically between two microstrip probes with narrow line width as shown in Fig. 7(f). In this setup, quasi-transverse electromagnetic wave was excited and received at the other end above 2 GHz with low-input return loss. As a result, the full measured PCJ transmission response was obtained. The measured signal isolation between two microwave probes is higher with the proposed PCJ than without it, indicating the PCJ's effectiveness in rejecting signal.

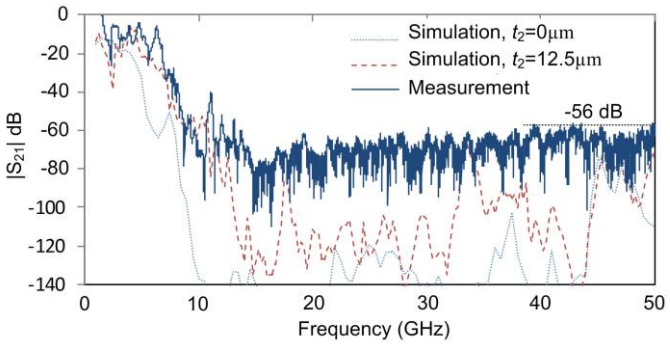

Fig. 9. The calibrated transmission measurement of pseudo plane wave propagation through the proposed PCJ.

V. Wavguide Flange Realization

The proposed PCJ with wide stop-band (version 2) was applied on one flange surface for a circular waveguide as a demonstration of functionality in Fig. 10. The circular waveguide with diameter of 1.538 mm, has a cutoff frequency equation to that of WR5.1. In this application, it also provides a non-contacting interface where space between the surfaces can be used to house planar circuits. Two flanges are separated by 6.4 µm in vacuum dielectric. The structure's dimension is scaled according to the cut-off waveguide frequency with w=0.506mm and d=0.778 mm. The smallest conductive post is measured 63×63×63 µm^3 which is realizable in metal by direct computer numerical control machining or in silicon via chemical micro-machining [11]. In the simulation model, radiation boundary is applied around the waveguide flange to observe power dissipation, while the waveguide flanges are

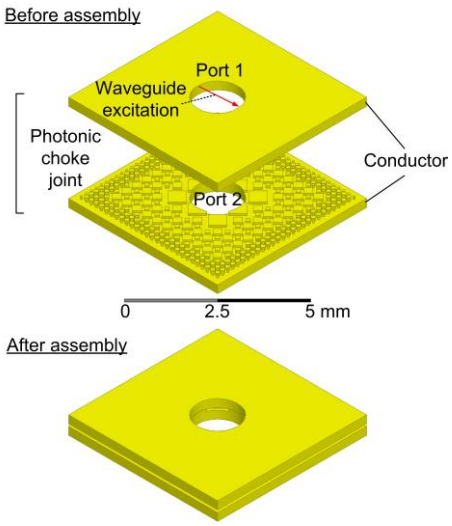

Fig. 10 The realization of the proposed PCJ pattern on as a WR5.1 circular waveguide flange.

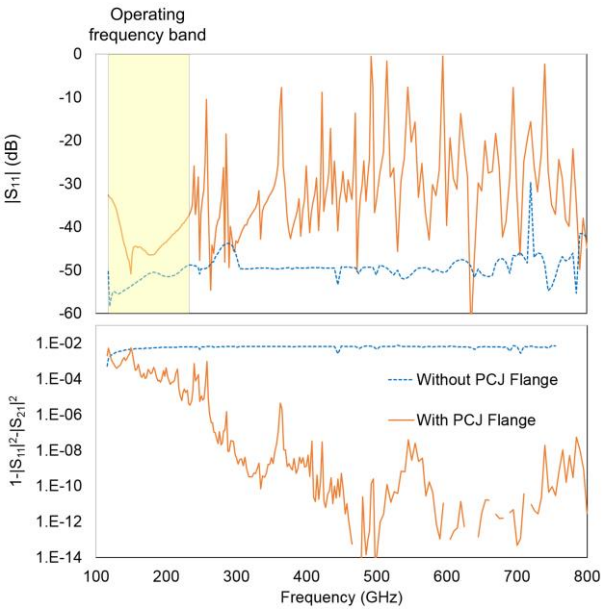

Fig. 11. The simulated circular waveguide flage input return loss (S_{11}) and power absorbsion ($1-|S_{11}|^2-|S_{21}|^2$), with and without the proposed PCJ. Both cases have a flange spacings of 6.4 µm.

made of perfect electric conductor. The ANSYS HFSS simulation results (in Fig. 11) show that the proposed waveguide flange provides significant reduction in in-band and out-of-band leakages in comparison to flat waveguide flange interface. The return loss of the proposed structure can be maintained above 30 dB from 118 to 238 GHz – demonstrating its low-loss full waveguide band transmission.

VI. Conclusion

A new photonic choke joint structure with sub-array Cartesian-tiling pillars was developed. The structure reduces the interface sensitivity and mating tolerances relative to a traditional planar interface while enabling new functionality. The PCJ design was validated with a pair of microstrip-to-pseudo-parallel-plate mode converters on a 25.4µm thick dielectric. The thin film dielectric layer was used to reduce the required spacer thickness and was observed to improve the isolation performance in the scale model. As a millimeter waveguide joint, the device provides broadband stop-band rejection and low in-band return loss.

References

[1] J. D. Joannopoulos, S. G. Johnson, J. N. Winn and R. D. Meade, Photonic Crystals: Molding the Flow of Light, Princeton University Press, 2008.

[2] T. Kamgaing and O. M. Ramahi, "Multiband electromagnetic-bandgap structures for applications in small form-Factor multichip module packages," IEEE Tran. Microwave Theory & Tech., vol.56, no.10, pp.2293-2300, October 2008.

[3] J. J. Simpson, A. Taflove, J. A. Mix, H. Heck, "Computational and experimental study of a microwave electromagnetic bandgap structure with waveguiding defect for potential use as a bandpass wireless interconnect," IEEE Microwave Wireless Compon. Lett., vol.14, no.7, pp.343,345, July 2004.

[4] R. E. Collin, Field Theory of Guided Waves, IEEE Press Ser. on Electromagn. Wave Theory, Wiley-IEEE, 1990.

[5] E. J. Wollack, K. U-yen and D.T. Chuss, "Photonic choke-joints for dual-polarization waveguides," 2010 IEEE MTT-S, pp. 177-180, May 2010.

[6] J. L. Hesler, "A photonic crystal joint (PCJ) for metal waveguide," 2001 IEEE MTT-S., vol. 2, pp. 783-786, May 2001.

[7] E. D. Sharp, "A high-power wide-band waffle-iron filter," IEEE Tran. Microwave Theory & Tech., vol. 11, no. 2, pp. 111-116, March 1963.

[8] K. Rostem, C. L. Bennett, D. T. Chuss, N. Costen, E. Crowe, K. L. Denis, J. R. Eimer, N. Lourie, T. Essinger-Hileman, T. A. Marriage, S. H. Moseley, T. R. Stevenson, D. W. Towner, G. Voellmer, E. J. Wollack, L. Zeng , "Detector architecture of the cosmology large angular scale surveyor," Proc. SPIE, vol. 8452, pp. 84521N-1-84521N-7, September 2012.

[9] S. J. Voeten, M. F. J. Vermeulen, G. J. H. Brussaard, A. J. M. Pemen, "Parallel plate transmission line transformer," 2011 IEEE Pulsed Power Conf., pp.303-306, June 2011.

[10] R. P. Hecken, "A near-optimum matching section without discontinuities," IEEE Tran. Microwave Theory & Tech, vol. 20, no. 11, pp. 734-739, November 1972.

[11] E. J. Crowe, C. L. Bennett, D. T. Chuss, K. L. Denis, J. Eimer, N. Lourie, T. Marriage, S. H. Moseley, K. Rostem, T. R. Stevenson, D. Towner, K. U-yen, E. J. Wollack, "Fabrication of a silicon backshort assembly for waveguide-coupled superconducting detectors,", IEEE Tran. Appl. Supercond., vol.23, no.3, pp.2500505, Jun. 2013.